Biophysical Reports

LETTER

Comparing confocal and two-photon Ca^{2+} imaging of thin low-scattering preparations

Jinbo Cheng,[1] Shane M. McMahon,[1] David W. Piston,[2] and Meyer B. Jackson[1]
[1]Department of Neuroscience, University of Wisconsin, Madison, Wisconsin and [2]Department of Cell Biology and Physiology, Washington University, St Louis, Missouri

ABSTRACT Ca^{2+} imaging provides insight into biological processes ranging from subcellular dynamics to neural network activity. Two-photon microscopy has assumed a dominant role in Ca^{2+} imaging. The longer wavelength infra-red illumination undergoes less scattering, and absorption is confined to the focal plane. Two-photon imaging can thus penetrate thick tissue ~10-fold more deeply than single-photon visible imaging to make two-photon microscopy an exceptionally powerful method for probing function in intact brain. However, two-photon excitation produces photobleaching and photodamage that increase very steeply with light intensity, limiting how strongly one can illuminate. In thin samples, illumination intensity can assume a dominant role in determining signal quality, raising the possibility that single-photon microscopy may be preferable. We therefore tested laser scanning single-photon and two-photon microscopy side by side with Ca^{2+} imaging in neuronal compartments at the surface of a brain slice. We optimized illumination intensity for each light source to obtain the brightest signal without photobleaching. Intracellular Ca^{2+} rises elicited by one action potential had twice the signal/noise ratio with confocal as with two-photon imaging in axons, were 31% higher in dendrites, and about the same in cell bodies. The superior performance of confocal imaging in finer neuronal processes likely reflects the dominance of shot noise when fluorescence is dim. Thus, when out-of-focus absorption and scattering are not issues, single-photon confocal imaging can yield better quality signals than two-photon microscopy.

WHY IT MATTERS Two-photon microscopy is widely favored in imaging studies of cellular calcium. However, photobleaching and photodamage by two-photon excitation have the potential to limit performance in thin samples. We tested laser scanning single-photon and two-photon fluorescent Ca^{2+} imaging side by side in neuronal processes at the surface of a brain slice, with illumination intensity optimized for each light source. Confocal microscopy produced a signal/noise ratio up to twice as high as two-photon microscopy in fine processes. Thus, single-photon confocal microscopy is the preferred method in imaging studies of fine processes in thin samples.

INTRODUCTION

Two-photon microscopy (2PM) is the method of choice for imaging cellular Ca^{2+}. Confinement of excitation to the focal plane and reduced scattering enable 2PM imaging in thick samples at depths ~10 times greater than with single-photon excitation. As a result, 2PM imaging with Ca^{2+} sensors has served as an exceptionally powerful method of studying functional activity in the brain (1–4). 2PM was initially thought to have an additional advantage of reduced photodamage and photobleaching (5–7). However, it is now well established that two-photon excitation produces steep nonlinear increases in photodamage, phototoxicity, and photobleaching (8–14). As a result of the large exponents of these destructive processes, they rise more steeply with illumination intensity than fluorescence emission, limiting the power that can be employed with 2PM. Higher illumination generally improves the signal/noise ratio (SNR) of photometric data because statistical fluctuations in photon number (shot noise) scale with the square root of excitation, whereas amplitudes scale linearly. The maximum nondestructive illumination power often optimizes SNR.

Steep rises in photo-destruction with illumination intensity have been reported for rhodamine and coumarin derivatives (8), Oregon Green BAPTA 1 (OGB1), Oregon

Shane M. McMahon's present address is Curi Bio, Seattle, Washington

Jinbo Cheng and Shane M. McMahon contributed equally to this work

Editor: Erdinc Sezgin.

https://doi.org/10.1016/j.bpr.2023.100109

Green BAPTA 2, Mg-green, fluorescein (9), Indo-I, NADH, aminocoumarin (10), fura-2 (11), Hoechst 33342 (13), and green and red fluorescent protein (12–14). In no instance was a fluorophore tested and found not to exhibit this behavior. The potential of photodamage to compromise performance of 2PM in thin samples has been noted (15–17). Yet, there is a widespread tendency for investigators to favor 2PM in virtually all forms of physiological imaging. To the best of our knowledge, experiments have not directly compared the performances of 2PM and single-photon confocal microscopy in thin samples. As a result, investigators lack a clear basis for choosing a method and often purchase a much more expensive 2PM. To address these issues, we evaluated 2PM and single-photon confocal microscopy in the same sample and setup. Ca^{2+} imaging was performed in patch-clamped neurons in hippocampal slices, focusing on processes close to the slice surface to achieve a thin-sample condition. In neurons loaded with the widely used Ca^{2+} indicator OGB1 (9), action potentials increased fluorescence in axons, dendrites, and somata. With illumination optimized for each light source, and with data from the same subcellular location, confocal microscopy produced a higher SNR than 2PM in finer neuronal processes, and a comparable SNR in larger nerve cell bodies.

MATERIALS AND METHODS

Images were acquired with a modified Ultima Multiphoton system (Bruker Corporation), coupled to an Olympus BX61 microscope, under control of Prairieview software (Bruker) (Fig. 1 *A*). A Coherent Chameleon Ti-Sapphire laser supplied 820-nm <200-fs pulses. Illumination was controlled by a Conoptics Pockel cell, with 10% directed to a power meter for monitoring. IR light was routed to a 775-nm short-pass dichroic mirror (DM1 in Fig. 1 *A*, Chroma ZT775sp-2p-UF1) and reflected into the galvanometer-controlled scanhead. Light then passed through a 660-nm long-pass dichroic mirror in the filter turret and through the objective (Olympus 60x LUMPlanFI/IR objective, NA 0.90, water immersion) to the sample. Confocal excitation light was supplied by a Laserboxx 488-nm diode laser (Oxxius), controlled by a Pockel cell, and coupled to a fiber port (Thorlabs CFC11A-A) through a neutral density filter (OD = 1) to a 499-nm dichroic mirror (DM2 in Fig. 1 *A*, Thorlabs MD499), through a 775-nm short-pass dichroic mirror (DM1), reflected into the scanhead, through the filter turret (set to an empty position for confocal), and into the objective.

Light was detected using two Hamamatsu H7422P-40 GaAsP photomultipliers (PMT), one for 2PM and the other for either 2PM or confocal (Fig. 1 *A*). For 2PM, nondescanned fluorescence was reflected by the 660-nm dichroic in the turret, through a 470- to 550-nm filter (Chroma), and into PMT2. Confocal epifluorescent light was descanned and passed through DM1 and DM2 into a pinhole (Thorlabs MPH16) set to 200 μm (~3 AU). Light was re-collimated by an aspheric lens and passed through a 500-nm long-pass filter (Thorlabs FELH0500) to PMT1. Alternatively, we performed 2PM with the turret in the empty position, so emitted light went to the scan head through the confocal pathway to PMT1, with the maximum pinhole setting of 2 mm. To switch between 2PM and confocal while a patch-clamp recording was in progress, the appropriate light source was selected with the Pockel cells, and the turret rotated into the appropriate position. Both were used for the same location, and the order varied randomly.

For both microscopies, illumination was increased in small increments (0.4 mW for 2PM and 0.07 μW for confocal) until photobleaching could be seen in a neuronal process, judged by noticeably reduced brightness in a 500-msec line scan. Power was then reduced to the maximum with undetectable photobleaching. The photobleaching threshold was especially clear in 2PM, so this optimization could be performed accurately. The increase in photobleaching was gradual with confocal microscopy, and we made this adjustment conservatively with lower illumination intensity. Optimal illumination levels were relatively similar across cells for each laser. The optimized power at the sample was 4.2–5 mW for 2PM and 0.22–0.36 μW for confocal microscopy (measured with a Thorlabs S170C power meter). The same power was used in measurements from axons, dendrites, and somata.

Ca^{2+} imaging was performed in patch-clamped dentate gyrus granule cells in hippocampal slices (18). Following a protocol approved by the UW ACUC, 3- to 4-week-old Sprague-Dawley rats were rendered unconscious with CO_2 and decapitated, the brain removed, and horizontal hippocampal slices (300 μm) cut with a Leica VT1200S vibratome in ice-cold cutting solution (in mM, 120 NaCl, 4 KCl, 25 $NaHCO_3$, 1.25 NaH_2PO_4, 3 Myo-inositol, 2 Na-pyruvate, 0.4 ascorbic acid, 3 $MgSO_4$, 0.1 $CaCl_2$, and 20 glucose) bubbled with 95% O_2/5% CO_2. Brain slices were incubated at 34°C for 30 min and kept at room temperature (~22°C) for another 30 min before recording. During recordings, slices were perfused with artificial cerebrospinal fluid (in mM, 125 NaCl, 4 KCl, 1.25 NaH_2PO_4, 26 $NaHCO_3$, 1 $MgSO_4$, 2 $CaCl_2$, and 10 glucose) bubbled with 95% O_2/5% CO_2 at room temperature. Neurons were patch-clamped with an Axopatch 200B amplifier and borosilicate glass patch pipettes (resistances 5–8 MΩ when filled with (in mM) 140 KCl, 2 NaCl, 4 $MgCl_2$, 4 Na-ATP, 10 HEPES, and 0.05 OGB1 (ThermoFisher), pH 7.3). Neurons were found under gradient contrast illumination and patch-clamped. Single action potentials were evoked by 1-msec current pulses under current clamp, and line scans were acquired at 0.95–1.08 kHz.

RESULTS

After establishing a whole-cell recording, OGB1 diffused from the patch pipette into the neuron, filling processes in ~15–30 min. Processes were generally close to the slice surface, so tissue scattering did not erode fluorescence. Fig. 1 *B* shows a 2PM *Z*-stack of a dye-filled soma, with axon above and dendrites below. *Z*-stacks are also shown of axons (Fig. 1 *C1*, 2PM; Fig. 2 *C2*, confocal) and dendrites (Fig. 2 *D1*, 2PM; Fig. 2 *D2*, confocal). Axons were thinner than dendrites, and process widths were similar between the two techniques, which have similar spatial resolutions due to cancellation of beam width halving and wavelength doubling in 2PM versus confocal microscopy (15,16). Confocal images were somewhat brighter than 2PM images (ratio 1.7 ± 0.3, n = 6) after adjusting illumination below the photobleaching threshold. Background light was higher with confocal microscopy than 2PM by 3.1 ± 1.7 (n = 6).

Fig. 2 *A1* shows an axon under confocal illumination with a line through a bouton. Scanning along this line

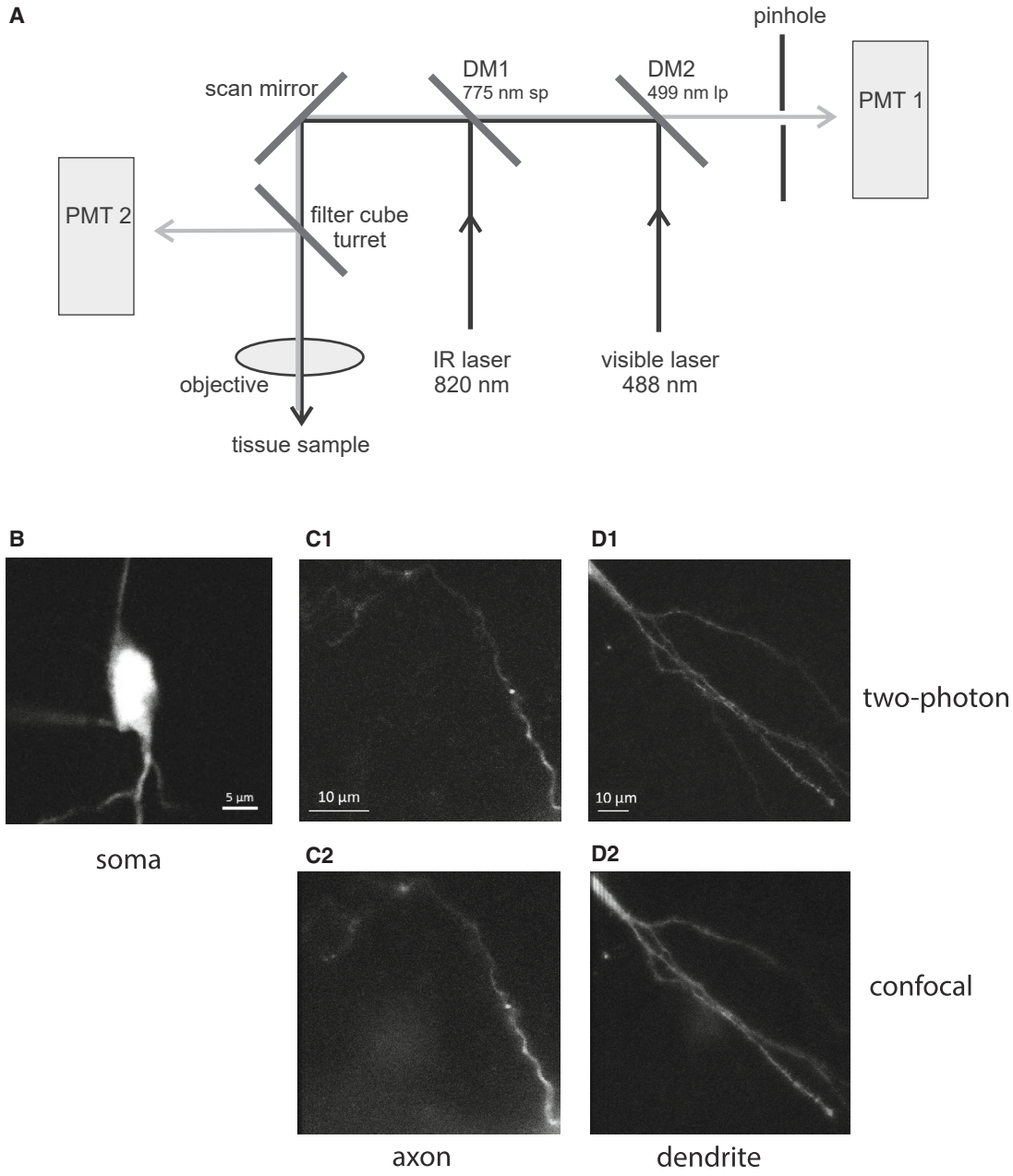

FIG. 1 (*A*) Light paths for 2PM and confocal microscopy (*black*, excitation; *gray*, emission). For 2PM, 820-nm light is reflected by DM1 to the scanhead, into the turret, the objective, and to the sample. Nondescanned emitted light is reflected in the turret to PMT2. For confocal microscopy, 488-nm light was reflected by DM2, through DM1, into the scanhead, the empty turret, the objective, and sample. Emitted light was directed to the scanhead, through DM1 and DM2 to a pinhole (set to 200 μm), and to PMT1. In 2PM, the turret could also be selected to direct light to the scanhead and PMT1 (pinhole, 2 mm). (*B*) 2PM image of a granule cell soma filled with OGB1. (*C1*) An OGB1-filled axon from a *Z*-stack projection using 2PM. (*C2*) The same axon in confocal microscopy. (*D1*) A dendrite in 2PM and (*D2*) in confocal microscopy. All images normalized to their maxima.

revealed a rise in fluorescence after eliciting an action potential (indicated by an arrow). Ca^{2+} entered the bouton and elevated [Ca^{2+}] by ~200 nM (18). Fluorescence was averaged over scanned lines and plotted versus time. The rise peaks <10 msec after the action potential. Ca^{2+} returns to baseline as Ca^{2+} is removed in boutons (Fig. 2 *B1* and *C1*), dendrites (Fig. 2 *B2* and *C2*), and somata (Fig. 2 *B3*, *C3*) with decay times of 100–200 msec. In each instance, confocal microscopy and 2PM were displayed from the same location so that the signal quality can be compared in a pairwise fashion.

The SNR was determined by dividing peak fluorescence rise above baseline (background subtracted)

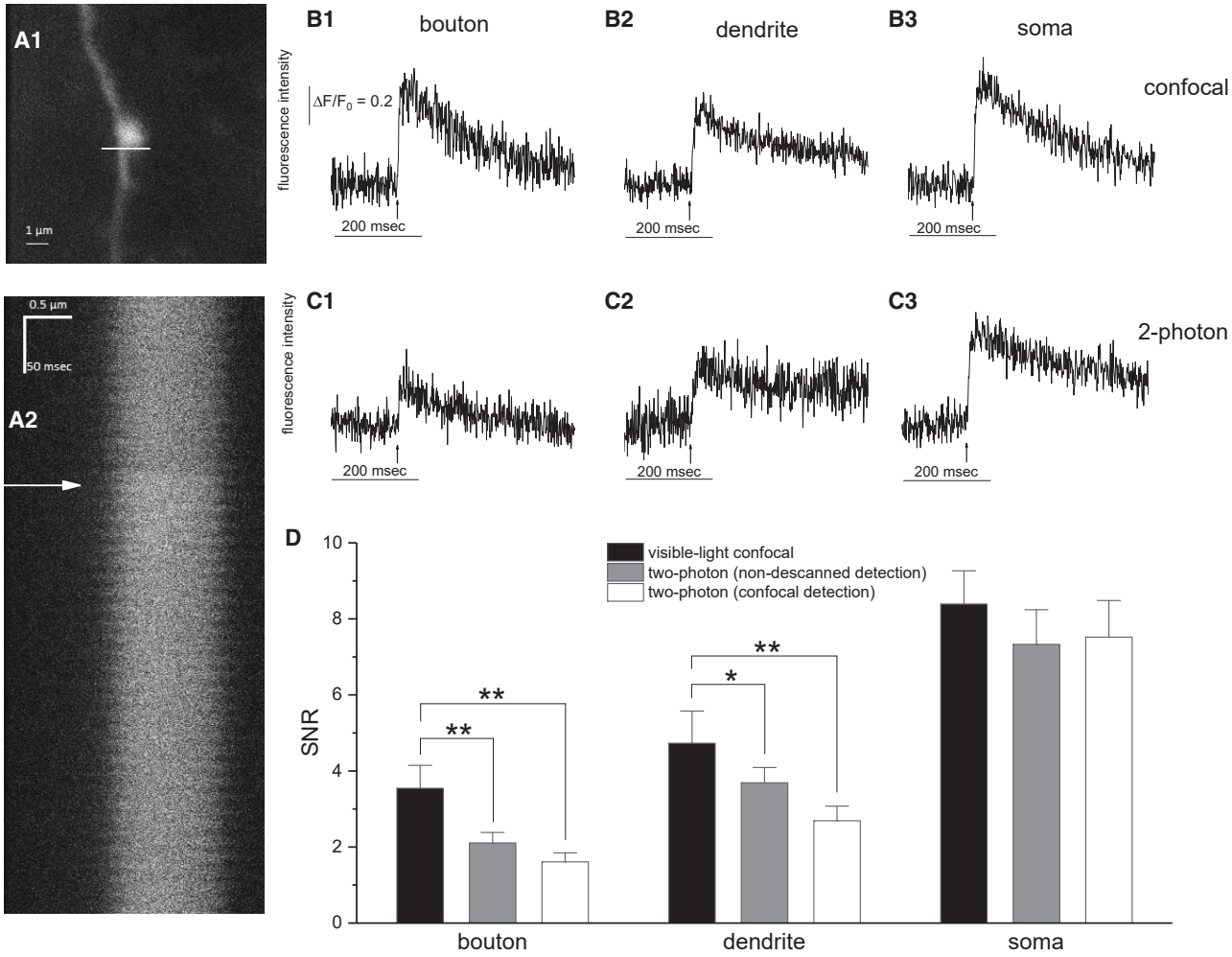

FIG. 2 (*A1*) Confocal image of axon and bouton, with white line selected for scanning. (*A2*). Line scans show fluorescence versus time, increasing following an action potential (*white arrow*). With confocal microscopy, line-scanned fluorescence (arbitrary units) was averaged through a bouton (*B1*), dendrite (*B2*), or soma (*B3*) and plotted versus time. Action potentials were evoked at arrows. 2PM in the same bouton (*C1*), dendrite (*C2*), or soma (*C3*). Fluorescence rose after action potentials (arrows). The $\Delta F/F_0$ scale applies to all panels. (*D*) Comparison of SNR between confocal microscopy and 2PM, with nondescanned and descanned 2PM detection (materials and methods; Fig. 1 *A*). Recordings were made pairwise in the same compartment, alternating between confocal microscopy and 2PM (12 boutons, 11 dendrites, 11 somata; mean ± SE, *p < 0.05, **p < 0.01, one-tailed paired *t*-test).

by the root-mean-square fluorescence of the prestimulus baseline (Fig. 2 *D*). To compare using the same detector, we also directed 2PM emission to the scan head and PMT1 (Fig. 1 *A*). The SNR ratio for confocal microscopy (PMT1) was nearly double that for nondescanned 2PM in boutons (PMT2), 31% higher in dendrites, and about the same in somata. With 2PM nondescanned detection, we saw a slightly higher SNR than descanned detection and PMT1. The SNR was highest for soma, lower for dendrites, and lowest for boutons. The general trend from these results is that confocal microscopy produces better signal quality than 2PM in recordings from finer processes. As expected, the SNR was greater for larger structures because of the larger fluorophore number.

DISCUSSION

This study compared confocal microscopy and 2PM in imaging of Ca^{2+} dynamics under thin-sample conditions where tissue absorption and scattering are negligible. Switching between the two forms of microscopy in recordings from the same subcellular compartment, using similar optical paths, and the same detectors facilitated the comparison. We also compared two optical detection pathways in 2PM, one of which was essentially identical to that used for confocal microscopy. In dentate gyrus neurons (granule cells) loaded with OGB1 (9,18), we found that single-photon confocal microscopy produced an SNR of up to twice that of 2PM with optimized illumination intensity. The difference was clear in finer processes (<2 μm) and

insignificant in large cell bodies (~10 μm). The greater difference between the two techniques with finer processes reflects the dimmer fluorescence, shorter scanned lines, and fewer fluorophores. Under these conditions, photon shot noise dominates. With larger structures and more emitted light, instrumentation takes over as the predominant noise source. With fine processes, one has the greatest incentive to increase illumination intensity, and this is where the reduced destruction with single-photon excitation has the greatest benefit. In larger cells than those tested here (>10 μm), optimized illumination 2PM may produce a better SNR than confocal microscopy.

We conducted this comparison with a widely used Ca^{2+}-sensitive fluorescent dye, OGB1. The relative performance of the two microscopies will likely vary with choice of fluorophore. GFP exhibits a higher order increase in photobleaching with intensity (12), which is worse at longer wavelengths (13). Thus, the advantages of confocal microscopy with GFP-based probes, including genetically encoded Ca^{2+} sensors, are likely to be greater. The points illustrated in the present study of Ca^{2+} should be relevant to imaging with fluorescent probes for other species, including Na^{+} (19), cAMP (20), and ATP (21).

It is hoped that the analysis provided here will aid investigators in the choice of method for the study of cellular dynamics. Confocal microscopy has the advantage of allowing stronger excitation due to lower destruction. Strategies such as passive pulse splitters can maximize intensity for each two-photon pulse, and this can significantly reduce photobleaching in some cases (22,23). This can improve the SNR in 2PM, but it also reduces the per sample signal level, introducing a trade-off between SNR and acquisition speed. These additional complications with 2PM are not issues with confocal imaging.

2PM is currently the only light microscopy technique capable of imaging hundreds of micrometers below the surface in intact tissue. Thus, 2PM must be used in order to study dynamic physiological processes deep within live preparations. However, when tissue penetration is not an issue the present results indicate that confocal imaging can perform better than 2PM, especially in fine processes. This was demonstrated here with neuronal processes at the surface of a brain slice. In cultured cells, the conditions will be better, so confocal microscopy may have a greater advantage. Widefield fluorescence may also be sufficient when rapid acquisition enabled with line scanning is not necessary. 2PM is more expensive than confocal microscopy due to the high cost of a Ti-sapphire laser. Less expensive femtosecond fiber lasers have been used for Ca^{2+} imaging (24) but are limited to a single wavelength. Tunable versions have been developed but may be more expensive if commercialized. In summary, for imaging Ca^{2+} with OGB1 in neuronal processes, confocal imaging performs as well as or better that 2PM, and it may also be preferable in other experiments when light scattering, out-of-focus absorption, and tissue penetration are not issues.

AUTHOR CONTRIBUTIONS

J.C. performed the experiments and analyzed the data. S.M.M. built the instrumentation. All authors contributed to design of experiments and the writing and editing of the paper.

ACKNOWLEDGMENTS

We thank Robert Fettiplace and Raunak Sinha for comments on the manuscript. This work was funded by NIH grants R01 NS103206 and R35 NS127219 to M.B.J. and R01 DK123301 to D.W.P.

DECLARATION OF INTERESTS

The authors declare no competing interests.

REFERENCES

1. Grienberger, C., A. Giovannucci, …, C. Portera-Cailliau. 2022. Two-photon calcium imaging of neuronal activity. *Nat. Rev. Methods Primers.* 2:67.
2. Jia, H., N. L. Rochefort, …, A. Konnerth. 2011. In vivo two-photon imaging of sensory-evoked dendritic calcium signals in cortical neurons. *Nat. Protoc.* 6:28–35.
3. Ohki, K., S. Chung, …, R. C. Reid. 2005. Functional imaging with cellular resolution reveals precise micro-architecture in visual cortex. *Nature.* 433:597–603.
4. Stosiek, C., O. Garaschuk, …, A. Konnerth. 2003. In vivo two-photon calcium imaging of neuronal networks. *Proc. Natl. Acad. Sci. USA.* 100:7319–7324.
5. Denk, W., J. H. Strickler, and W. W. Webb. 1990. Two-photon laser scanning fluorescence microscopy. *Science.* 248:73–76.
6. Potter, S. M. 1996. Vital imaging: two photons are better than one. *Curr. Biol.* 6:1595–1598.
7. Denk, W., and K. Svoboda. 1997. Photon upmanship: why multiphoton imaging is more than a gimmick. *Neuron.* 18:351–357.
8. Eggeling, C., J. Widengren, …, C. A. Seidel. 1998. Photobleaching of Fluorescent Dyes under Conditions Used for Single-Molecule Detection: Evidence of Two-Step Photolysis. *Anal. Chem.* 70:2651–2659.
9. Koester, H. J., D. Baur, …, S. W. Hell. 1999. Ca2+ fluorescence imaging with pico- and femtosecond two-photon excitation: signal and photodamage. *Biophys. J.* 77:2226–2236.
10. Patterson, G. H., and D. W. Piston. 2000. Photobleaching in two-photon excitation microscopy. *Biophys. J.* 78:2159–2162.
11. Hopt, A., and E. Neher. 2001. Highly nonlinear photodamage in two-photon fluorescence microscopy. *Biophys. J.* 80: 2029–2036.
12. Chen, T. S., S. Q. Zeng, …, W. Zhou. 2002. High-order photobleaching of green fluorescent protein inside live cells in two-photon excitation microscopy. *Biochem. Biophys. Res. Commun.* 291:1272–1275.

13. Kalies, S., K. Kuetemeyer, and A. Heisterkamp. 2011. Mechanisms of high-order photobleaching and its relationship to intracellular ablation. *Biomed. Opt Express.* 2:805–816.

14. Drobizhev, M., R. S. Molina, and J. Franklin. 2022. Multiphoton Bleaching of Red Fluorescent Proteins and the Ways to Reduce It. *Int. J. Mol. Sci.* 23, 770.

15. Denk, W. 1996. Two-photon excitation in functional biological imaging. *J. Biomed. Opt.* 1:296–304.

16. Denk, W., D. W. Piston, and W. W. Webb. 2006. Multi-photon molecular excitation in laser-scanning microscopy. *In* Handbook of Biological Confocal Microscopy. J. B. Pawley, ed. Springer, New York, pp. 535–549.

17. Piston, D. W. 2017. Two-Photon Excitation Microscopy for Three-Dimensional Imaging of Living Intact Tissues. *In* Fluorescence Microscopy: From Principles to Biological Applications. U. Kubitscheck, ed. Wiley-VCH Verlag, pp. 204–242.

18. Jackson, M. B., and S. J. Redman. 2003. Calcium dynamics, buffering, and buffer saturation in the boutons of dentate granule-cell axons in the hilus. *J. Neurosci.* 23:1612–1621.

19. Miyazaki, K., and W. N. Ross. 2022. Fast synaptically activated calcium and sodium kinetics in hippocampal pyramidal neuron dendritic spines. *eNeuro.* 9. ENEURO.0396-22.2022.

20. DiPilato, L. M., X. Cheng, and J. Zhang. 2004. Fluorescent indicators of cAMP and Epac activation reveal differential dynamics of cAMP signaling within discrete subcellular compartments. *Proc. Natl. Acad. Sci. USA.* 101:16513–16518.

21. Rangaraju, V., N. Calloway, and T. A. Ryan. 2014. Activity-driven local ATP synthesis is required for synaptic function. *Cell.* 156:825–835.

22. Dittrich, P., F. Malvezzi-Campeggi, …, P. Schwille. 2001. Accessing molecular dynamics in cells by fluorescence correlation spectroscopy. *Biol. Chem.* 382:491–494.

23. Mütze, J., V. Iyer, …, T. D. Harris. 2012. Excitation spectra and brightness optimization of two-photon excited probes. *Biophys. J.* 102:934–944.

24. Ricken, S., J. Leipziger, …, R. Nitschke. 1998. Simultaneous measurements of cytosolic and mitochondrial Ca2+ transients in HT29 cells. *J. Biol. Chem.* 273:34961–34969.